Cell, Vol. 114, 673–688, September 19, 2003, Copyright ©2003 by Cell Press

Involvement of Histone H1.2 in Apoptosis Induced by DNA Double-Strand Breaks

Akimitsu Konishi,[1,6,8] Shigeomi Shimizu,[1,2,3,8] Junko Hirota,[4] Toshifumi Takao,[4] Yuhong Fan,[7] Yosuke Matsuoka,[5] Lilin Zhang,[1,3] Yoshihiro Yoneda,[5] Yoshitaka Fujii,[6] Arthur I. Skoultchi,[7] and Yoshihide Tsujimoto[1,2,3,*]

[1]Department of Post-Genomics and Diseases
Osaka University Medical School
[2]CREST and
[3]SORST of the Japan Science and Technology Corporation (JST)
[4]Institute for Protein Research
Osaka University
[5]Department of Frontier Biosciences
Graduate School of Frontier Biosciences
Osaka University
2-2 Yamadaoka, Suita
Osaka 565-0871
Japan
[6]Department of Surgery II
Nagoya City University Medical School and
Graduate School of Medical Sciences
1 Kawasumi
Nagoya 467-8601
Japan
[7]Department of Cell Biology
Albert Einstein College of Medicine
Bronx, New York 10461

Summary

It is poorly understood how apoptotic signals arising from DNA damage are transmitted to mitochondria, which release apoptogenic factors into the cytoplasm that activate downstream destruction programs. Here, we identify histone H1.2 as a cytochrome c-releasing factor that appears in the cytoplasm after exposure to X-ray irradiation. While all nuclear histone H1 forms are released into the cytoplasm in a p53-dependent manner after irradiation, only H1.2, but not other H1 forms, induced cytochrome c release from isolated mitochondria in a Bak-dependent manner. Reducing H1.2 expression enhanced cellular resistance to apoptosis induced by X-ray irradiation or etoposide, but not that induced by other stimuli including TNF-α and UV irradiation. H1.2-deficient mice exhibited increased cellular resistance in thymocytes and the small intestine to X-ray-induced apoptosis. These results indicate that histone H1.2 plays an important role in transmitting apoptotic signals from the nucleus to the mitochondria following DNA double-strand breaks.

Introduction

Apoptosis plays an important role in various biological events in metazoans including development, maintenance of tissue homeostasis, and elimination of harmful cells. The process of apoptosis is driven by a family of cysteine proteases called caspases, which cleave various cellular proteins to cause apoptotic death. It has been shown that the mitochondria play a crucial role in apoptosis by releasing several apoptogenic molecules (such as cytochrome c, Smac/DIABLO, Omi/HtrA2, AIF, and endonuclease G) into the cytoplasm from the intermembrane space; these molecules activate downstream destruction programs including the caspase cascade (reviewed by Wang, 2001; Wolf and Green, 2002).

The best-characterized regulators of apoptosis are the Bcl-2 family of proteins, which directly modulate outer mitochondrial membrane permeability during apoptosis. This family of proteins comprises anti-apoptotic members such as Bcl-2 and Bcl-xL, as well as proapoptotic members like multidomain Bax or Bak and numerous single-domain BH3-only proteins (reviewed by Adams and Cory, 1998; Tsujimoto and Shimizu, 2000; Tsujimoto, 2003). Many of the proapoptotic family members (including Bax and BH3-only proteins such as Bid, Bad, Bim, and Bmf) are localized in the cytoplasm of living cells. Apoptotic stimulation causes both translocation of these proteins to the mitochondria and induction of membrane permeabilization, probably by inactivation of anti-apoptotic Bcl-2 family members and activation of multidomain members such as Bax and Bak (Antonsson et al., 2000, 2001; Wei et al., 2001). Various BH3-only proteins appear to be activated in a specific manner depending on the apoptotic stimulus and then translocate to the mitochondria (reviewed by Puthalakath and Strasser, 2002). For example, Bid is cleaved by caspase-8 in Fas/TNF receptor-mediated apoptosis, Bad is dephosphorylated and unleashed from 14-3-3 in Ca^{2+} overload-induced apoptosis, and Bmf and Bim are released from the cytoskeleton in anoikis and lymphokine deprivation-induced apoptosis, respectively (reviewed by Puthalakath and Strasser, 2002). Two BH3-only proteins (Noxa and Puma) have been reported to be involved in apoptosis due to DNA damage (Oda et al., 2000a; Nakano and Vousden, 2001). These proteins are transcriptionally activated by p53 during DNA damage-induced apoptosis. Bax has also been shown to be involved in DNA damage-induced apoptosis through transcriptional upregulation (Miyashita and Reed, 1995) as well as translocation to the mitochondrial membrane after a conformational change (Wolter et al., 1997; Gross et al., 1998). Non-Bcl-2 family members such as p53 (Marchenko et al., 2000), p53AIP1 (Oda et al., 2000b), nuclear orphan receptor TR3 (Li et al., 2000), and Peutz-Jegher gene product LKB1 (Karuman et al., 2001) also undergo translocation to the mitochondria and induce membrane permeabilization by still-unknown mechanisms. Some of these molecules might be functionally redundant and may show differential use in various cell types, but the mechanisms of signal transmission from the nucleus to the mitochondria during DNA damage-induced apoptosis are not fully understood.

In the present study, we took a different approach to

*Correspondence: tsujimot@gene.med.osaka-u.ac.jp
[8]These authors equally contributed to this work.

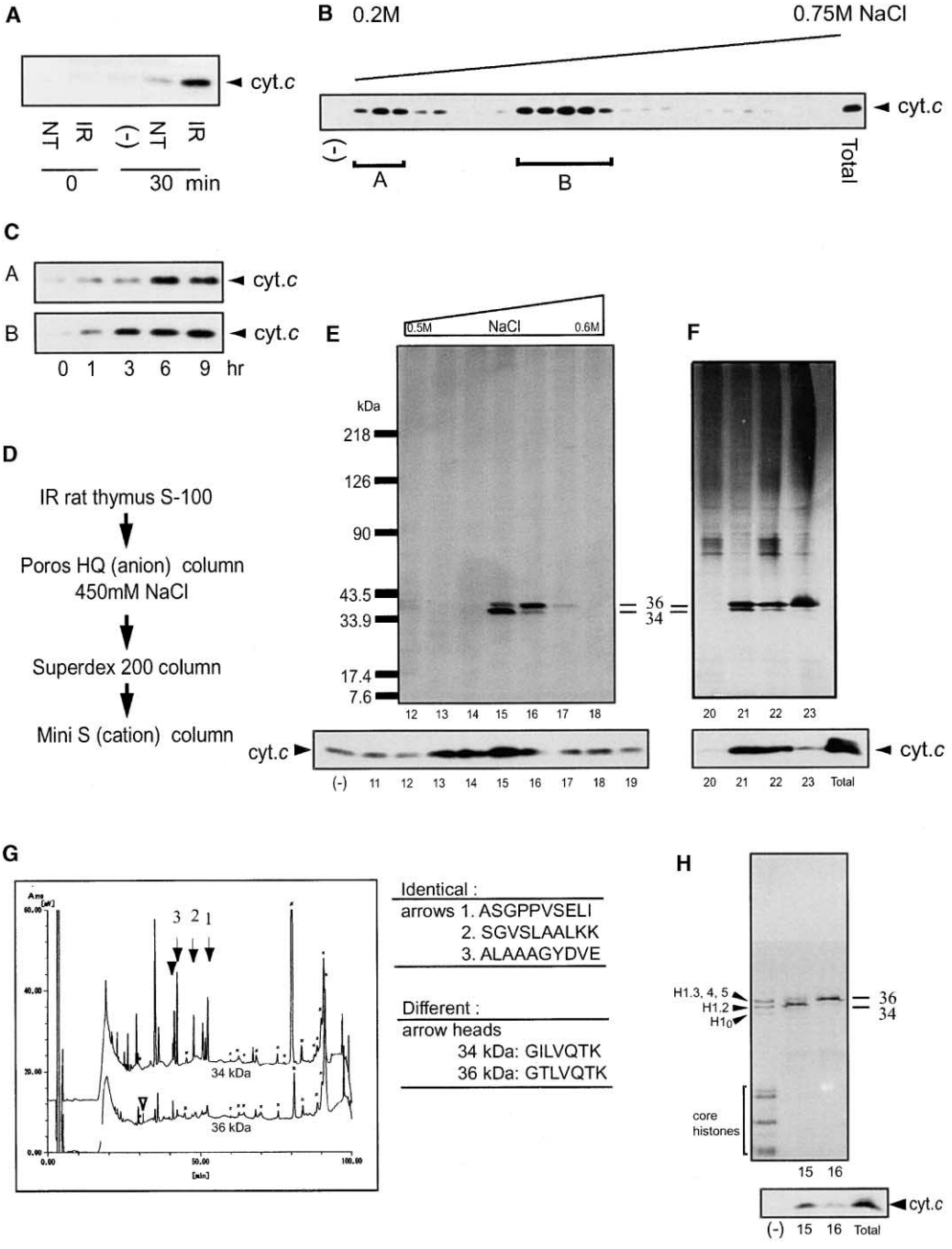

Figure 1. Purification of a Cytochrome c-Releasing Factor As Histone H1.2

(A) Presence of cytochrome c-releasing activity in X-ray-irradiated thymic cytosol. The cytosolic fraction was obtained from the thymus of a normal rat (NT) and from the thymus of a rat 3 hr after exposure to 20 Gy of X-ray irradiation (IR). Each cytosolic fraction (150 μg) was added to rat liver mitochondria (100 μg) for the indicated time. Mitochondria were also incubated alone (−). In the experiments here and below, the release of cytochrome c was assessed by Western blotting.

(B) Separation of cytochrome c-releasing activity by anion exchange column chromatography. Cytosolic fractions were obtained from thymi dissected 6 hr after rats were irradiated with X-rays (20 Gy) and were loaded onto a Poros HQ column. After proteins were eluted and desalted, they were incubated with isolated mitochondria (100 μg), and cytochrome c release was assessed. Mitochondria were also incubated alone (−). "Total" represents the total amount of cytochrome c in the same amount of mitochondria.

(C) Time-dependent increase of cytochrome c-releasing activity. Rat thymic cytosolic fractions were recovered at the indicated times after X-ray irradiation (20 Gy) and were loaded onto a Poros HQ column. Fractions corresponding to sections A and B in Figure 1B were desalted, incubated with isolated mitochondria, and assessed for the release of cytochrome c.

(D) Diagram of the purification method.

(E and F) Purification of cytochrome c-releasing factor from rat thymus. Fractions corresponding to section B in Figure 1B were loaded onto a Superdex 200 column followed by a Mini S column (E) or a Poros HS column (F). Aliquots (10 μl) of the indicated fractions were subjected

the identification of a signaling molecule involved in DNA damage-induced apoptosis by searching for a cytochrome c-releasing factor that appeared in the cytoplasm after X-ray irradiation of the thymus. As a result, we isolated histone 1.2, one of the linker histones. Histone H1 normally binds to the linker DNA between nucleosomes, sealing off two turns of DNA around a histone octamer, and is involved in the formation of higher-ordered chromatin structures and in the inhibition of transcription (reviewed by Vignali and Workman, 1998). Eight isotypes of histone H1 have been reported in mice (Wang et al., 1997; Tanaka et al., 2001) and humans (Albig and Doenecke, 1997). Among them, all of the somatic H1s (H1.1–H1.5) are ubiquitously expressed in all cell types (Lennox and Cohen, 1983). The present study demonstrates that histone H1.2, but not other histone H1 isotypes, possesses strong cytochrome c-releasing activity, and that histone H1.2 is released into the cytoplasm from the nucleus in response to DNA double-strand breaks, but not other apoptotic stimuli.

Results

Purification of an X-Ray-Induced Cytochrome c-Releasing Factor

To identify molecule(s) acting downstream of DNA damage that are responsible for inducing the release of apoptogenic cytochrome c from the mitochondria, we set up an in vitro assay system using isolated rat liver mitochondria and rat thymus cytosol. The cytosol, obtained from the thymus of rats subjected to whole-body X-ray irradiation, was capable of inducing cytochrome c release from the mitochondria (Figure 1A). After anion exchange chromatography, cytochrome c-releasing activity was detected in two fractions (fraction A at 0.25 M NaCl and fraction B at 0.45 M; Figure 1B). Although the activity of both fractions was increased by irradiation in a time-dependent manner (Figure 1C), the activity of fraction B was stronger than fraction A. Fraction A contained Bax (data not shown), which is known to induce cytochrome c release but is not essential for X-ray irradiation-induced death of thymocytes, because $Bax^{-/-}$ thymocytes and $Bax^{+/+}$ thymocytes are equally sensitive to X-ray irradiation (Knudson et al., 1995). We therefore tried to identify a cytochrome c-releasing factor in fraction B. Following the protocol described in Figure 1D, we identified a 34 kDa protein that was closely associated with cytochrome c-releasing activity (Figure 1E). No (or very weak) activity of the 36 kDa protein was confirmed by a different purification procedure using a cation exchange column (Poros HS) instead of Superdex 200 and Mini S (Figure 1F, lane 23).

To determine their amino acid sequences, the 34 and 36 kDa proteins were excised from a gel and subjected to trypsin digestion, and the resulting peptides were separated by reverse-phase HPLC. Unexpectedly, the peptide maps of the 34 and 36 kDa proteins were quite similar (Figure 1G), suggesting that these were the same protein with different modifications or else were two proteins from the same family. The sequences of three identical peptides and two different peptides (shown by arrows and arrowheads, respectively, in Figure 1G) were determined by Edman degradation. A database search revealed that the sequences of the three identical peptides ASGPPVSELI, SGVSLAALKK, and ALAAAGYDVE (Figure 1G, arrows 1–3) perfectly matched those of mouse histone H1.2 and H1.3. The sequence of the different 34 kDa peptide (indicated by the closed arrowhead) and that of the 36 kDa peptide (open arrowhead) were determined to be GILVQTK and GTLVQTK, respectively, matching the sequences of mouse histone H1.2 and H1.3, respectively. These results suggested that the 34 kDa protein with cytochrome c-releasing activity was rat histone H1.2. To determine whether mouse histone H1.2 also possessed cytochrome c-releasing activity, histone H1 was obtained from healthy mouse thymus (see Experimental Procedures). A fraction enriched in the 34 kDa protein and containing little of the 36 kDa protein caused substantial release of cytochrome c (Figure 1H, lane 15). Amino acid sequence analysis indicated that the 34 and 36 kDa proteins were mouse histone H1.2 and H1.3, respectively. Histone H1 consists of six forms (except for germline specific H1t and H1oo), which can be separated into three bands by SDS-PAGE ($H1_0$ at 32 kDa; H1.2 at 34 kDa; and a mixture of H1.3, H1.4, and H1.5 at 36 kDa [H1.1 was not rigorously analyzed]) (Chadee et al., 1997, and our unpublished results). Histone H1.3 was the major component of the 36 kDa protein from mouse thymus (see Figure 4D). Thus, like rat H1.2 (34 kDa), mouse H1.2 showed cytochrome c-releasing activity.

Release of Cytochrome c from Isolated Mitochondria by Recombinant Histone H1.2

To confirm the cytochrome c-releasing activity of histone H1.2, we generated recombinant mouse histone H1.2 (rH1.2) and H1.4 (Figure 2A). As shown in Figure 2B, rH1.2 possessed cytochrome c-releasing activity, but rH1.4 did not. Commercially available calf thymus histone H1 (containing H1.2, but not core histones) also induced cytochrome c release (Figure 2C). To confirm that histone H1.2 specifically possesses cytochrome c-releasing activity, histone H1 obtained from mouse thymus nuclei was further purified using reverse-phase HPLC (Figure 2D). Mass spectrometry of the proteins

to electrophoresis on 5%–20% gradient SDS-polyacrylamide gel, and proteins were visualized by silver staining (top). Aliquots (40 μl) of the same fractions were desalted and incubated with isolated mitochondria, and the release of cytochrome c was assessed (bottom).

(G) Peptide map of cytochrome c-releasing factor. The 34 and 36 kDa proteins (Figure 1E) were excised from a gel and subjected to trypsin digestion. The resulting peptides were separated by HPLC, and their amino acid sequences were determined. Arrows and arrowheads indicate identical and different peptides in the two proteins, respectively, and their amino acid sequences are shown on the right.

(H) Purification of cytochrome c-releasing factor from mouse thymus. Mouse histone H1 was purified as described in Experimental Procedures. Aliquots (10 μl) of the total acid extract (left lane) and of fractions 15 and 16 eluted from the Mini S column were subjected to 15% SDS-PAGE, after which the gel was stained (top). Aliquots (40 μl) of the same fractions were tested for the release of cytochrome c. Mitochondria were also incubated alone (−).

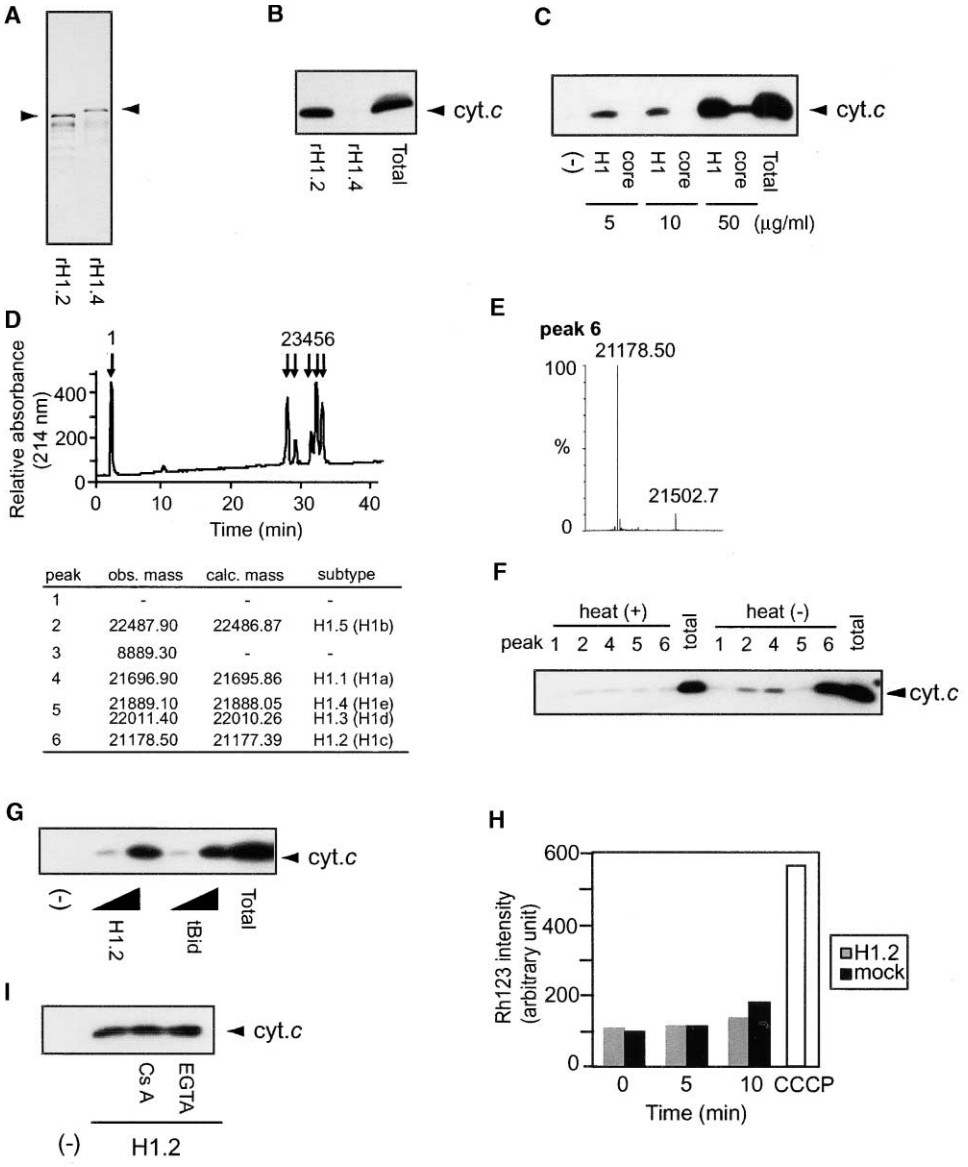

peak	obs. mass	calc. mass	subtype
1	-	-	-
2	22487.90	22486.87	H1.5 (H1b)
3	8889.30	-	-
4	21696.90	21695.86	H1.1 (H1a)
5	21889.10 22011.40	21888.05 22010.26	H1.4 (H1e) H1.3 (H1d)
6	21178.50	21177.39	H1.2 (H1c)

Figure 2. Histone H1.2 Induces Cytochrome c Release from Isolated Mitochondria

(A–C) Induction of cytochrome c release by recombinant histone H1.2. (A) Recombinant mouse histone H1.2 (rH1.2) and rH1.4 were separated on a 15% SDS-polyacrylamide gel and visualized by CBB staining. (B and C) rH1.2 and rH1.4 (30 μg/ml) (B) or calf histone H1 and core histones at the indicated concentrations (C) were incubated with isolated rat mitochondria, and the release of cytochrome c was assessed. "Total" represents the total amount of cytochrome c in the same amount of mitochondria.

(D–F) Induction of cytochrome c release by histone H1.2, but not other H1 isoforms. (D) Histone H1 was isolated by acid extraction of the nuclear fraction from mouse thymus and was separated by RP-HPLC (see Supplemental Experimental Procedures). Proteins were collected from all fractions showing peaks (numbered 1–6) and subjected to mass spectrometry. Based on the observed molecular masses, the histone H1 subtype of each peak was assigned as described in the table. (E) Mass spectrometric analysis of the protein in peak 6. (F) Each histone H1 subtype was collected, as well as a low molecular weight protein in peak 1, and TFA was removed. Then, an aliquot of each sample was heat-denatured (heat[+]). Next, the samples (the same amount of protein) were incubated with isolated rat mitochondria, and the release of cytochrome c was assessed. Numbers correspond to the peaks in (D).

(G) Cytochrome c-releasing activity of histone H1.2 is comparable to that of tBid. Isolated mitochondria (1 mg/ml) were incubated without (−) or with rH1.2 or rtBid at both 10 and 30 μg/ml.

(H) Cytochrome c release induced by histone H1.2 without loss of mitochondrial $\Delta\psi$. Mitochondria (1 mg/ml) were incubated with 50 μg/ml rH1.2 or mock protein, and $\Delta\psi$ was measured at the indicated time on the basis of rhodamine 123 uptake. CCCP (a protonophore; 1 mM for 15 min) was used as the control to completely dissipate $\Delta\psi$. Loss of $\Delta\psi$ caused the release of rhodamine 123 from the mitochondria, resulting in an increase of the rhodamine 123 intensity.

(I) Permeability transition inhibitors do not inhibit histone H1.2-induced cytochrome c release. Mitochondria (1 mg/ml) were incubated without (−) or with 50 μg/ml rH1.2 in the presence or absence of 1 μM CsA and 0.2 mM EGTA.

in all six fractions revealed that peaks 2, 4, 5, and 6 corresponded to various isoforms of histone H1 (Figures 2D and 2E). These histone H1s were recovered (i.e., TFA was removed) and assessed for cytochrome c-releasing activity. Only H1.2, but not the other isoforms, showed strong cytochrome c-releasing activity (Figure 2F), consistent with the results shown in Figure 1, although H1.5 and H1.1 showed some weak activity. These results indicated that histone H1.2 itself was able to release cytochrome c. Under our experimental conditions, the cytochrome c-releasing activity of histone H1.2 was comparable to that of a known cytochrome c-releasing factor, truncated Bid (Figure 2G).

Next, we examined whether histone H1.2-induced cytochrome c release was accompanied by the mitochondrial permeability transition (PT), which is characterized by loss of $\Delta\psi$ (the potential across the inner membrane; reviewed by Zoratti and Szabo, 1995). As shown in Figure 2H, histone H1.2 did not induce $\Delta\psi$ loss (assessed using rhodamine 123), whereas the ionophore CCCP caused complete dissipation of $\Delta\psi$. Furthermore, histone H1.2-induced cytochrome c release was not inhibited by two PT inhibitors, cyclosporin A and EGTA (Figure 2I). These results indicated that histone H1.2-induced cytochrome c release was a PT-independent process.

Involvement of Bak in Histone H1.2-Induced Cytochrome c Release

It was recently reported that cells from *bax/bak* double knockout mice are resistant to various apoptotic stimuli, including genotoxic stress, suggesting that Bax and Bak may act as a gateway for various apoptotic signals (Lindsten et al., 2000, Wei et al., 2001). It has also been suggested that Bax and Bak exist as inactive forms in cells, with apoptotic stimulation causing their activation through a conformational change and oligomerization (Desagher et al., 1999; Griffiths et al., 1999; Wei et al., 2000). We examined the effect of histone H1.2 on Bak in digitonin-permeabilized cells using a conformation-specific monoclonal antibody that only binds activated Bak. Immunofluorescence microscopy demonstrated that rH1.2 caused the activation of Bak in a concentration-dependent manner, like rBid, while rBcl-xL markedly inhibited Bak activation (Figure 3A). We observed concentration-dependent oligomerization of Bak in rH1.2-treated mitochondria, as with rBid (Figure 3B). Furthermore, when mitochondria were isolated from the livers of Bak-deficient mice with undetectable levels of Bax (data not shown), histone H1.2 did not induce cytochrome c release at a concentration below 50 μg/ml (Figure 3C). However, a higher concentration of histone H1.2 induced cytochrome c release in a Bak-independent manner (Figure 3C) without Bak oligomerization (data not shown), which might have been a nonspecific action of this histone. Consistent with the results shown in Figure 3A, rBcl-xL inhibited histone H1.2-induced cytochrome c release in rat liver mitochondria (Figure 3D). Taken together, these findings demonstrate that histone H1.2 can induce cytochrome c release in a Bak-dependent manner.

Cytoplasmic Increase of Histone H1.2 after X-Ray Irradiation

Histone H1 is not detected in the cytosol of thymocytes of a healthy mouse (Figure 4A) because histone H1 is synthesized in the cytoplasm and rapidly transported to the nucleus (Matsuoka et al., 1994; Vignali and Workman, 1998). After X-ray irradiation, however, histone H1.2 and other forms of histone H1 showed a time-dependent and X-ray dose-dependent increase in the cytosol (Figure 4A). Consistent with the above, immunostaining for histone H1 in healthy mouse embryonic fibroblasts (MEFs) revealed that this histone was only located in the nucleus, whereas it was also observed in the cytoplasm of X-ray-irradiated MEFs (Figure 4B), indicating that an increase in the cytoplasmic fraction occurred after X-ray irradiation.

Next, we examined whether cytoplasmic histone H1 was different from nuclear histone H1 in mouse thymus. The thymus cytosol of mice with and without X-ray irradiation and the nuclear fraction of nonirradiated thymus were subjected to acid extraction to purify histone H1. By reverse-phase HPLC, histone H1 was detected in the nuclear fraction of nonirradiated thymus and in the cytosolic fraction of X-ray-irradiated thymus, but not in the cytosolic fraction from nonirradiated thymus (Figure 4C), consistent with the results shown in Figure 4A. Cytosolic histone H1 reached 5%–10% of total histone content 3 hr after irradiation. Differences in HPLC profiles in Figure 4C and 2D were due to the different column size and gradient used. The H1 fractions were analyzed by mass spectroscopy (Figure 4D). The nuclear fraction of nonirradiated thymus contained five native histones (H1.1–H1.5), the observed mass of which was almost equal to the calculated mass (see Figure 2D, table). The cytosolic fraction from X-ray-irradiated thymus also contained the same H1 molecules as those seen in the nonirradiated nucleus. Note that a small fraction of histone H1 molecules are phosphorylated at multiple sites, which causes the molecular mass to increase by multiples of 80 as seen in multiple small peaks to the right of the major peaks (Figure 4D). Histone H1 did not show any X-ray irradiation-specific modifications (Figure 4D), a finding in agreement with the result that histone H1.2 from the nonirradiated nucleus showed cytochrome c-releasing activity (Figure 1H).

Role of p53 in the Cytoplasmic Increase of Histone H1

p53 is essential for DNA damage-induced apoptosis in many types of cells, and thymocytes from $p53^{-/-}$ mice are resistant to X-ray irradiation-induced apoptosis (Lowe et al., 1993a; Clarke et al., 1993). Therefore, we examined the relationship between p53 and histone H1.2. When $p53^{+/+}$, $^{+/-}$, and $^{-/-}$ mice were irradiated, cytochrome c release and caspase activation were seen in the thymus of $p53^{+/+}$ and $^{+/-}$ mice, but not in that of $p53^{-/-}$ mice (Figures 4E and 4F), as observed previously (Westphal et al., 1997). As shown in Figure 4E, histone H1.2 and other subtypes of histone H1 were increased in the cytosolic fraction from the thymus of $p53^{+/+}$ and $^{+/-}$ mice, whereas this increase was not observed in the thymus of $p53^{-/-}$ mice (Figure 4E). These results indicated that p53 is necessary for a cytoplasmic increase of various forms of histone H1, including H1.2.

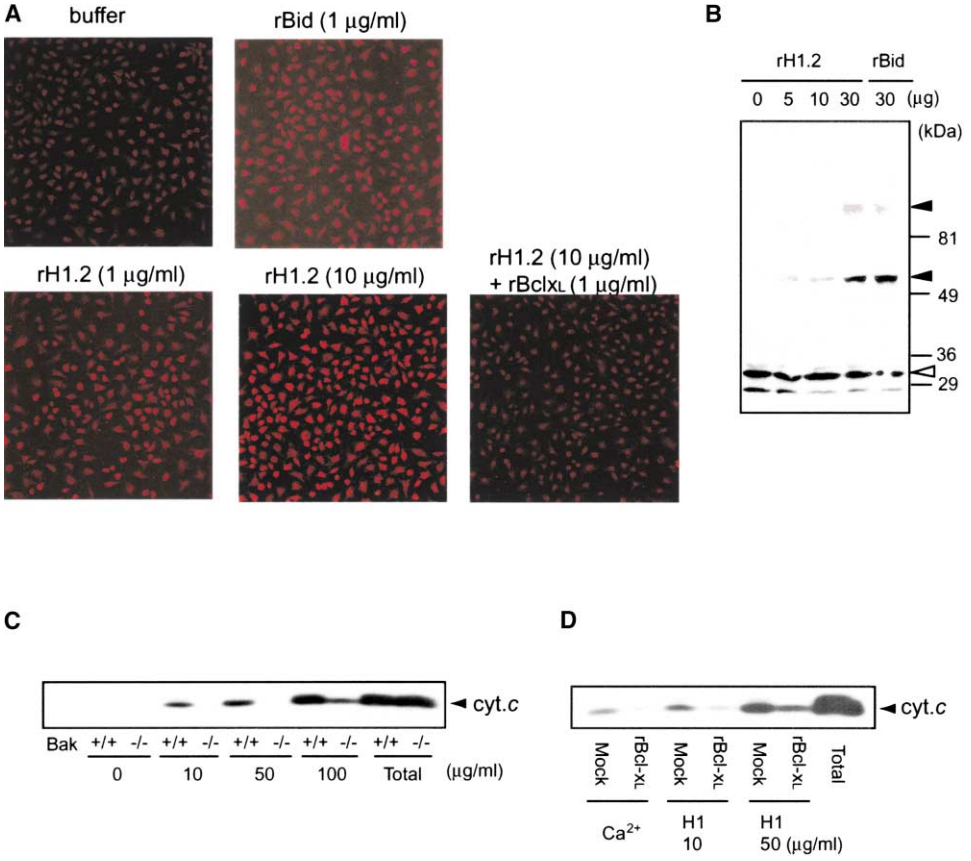

Figure 3. Bak-Dependence of Histone H1.2-Induced Cytochrome c Release

(A) Activation of Bak by rH1.2. HeLa cells were permeabilized with digitonin, and buffer or the indicated proteins were added for 10 min. The cells were then fixed with paraformaldehyde and stained with an antibody specific for active Bak (shown in red).

(B) Oligomerization of Bak by rH1.2. Isolated mitochondria (100 μg) were incubated with the indicated amount of rH1.2 and rtBid for 30 min, after which 10 mM BMH was added for 30 min. The mitochondria were then centrifuged and dissolved in 2× sample buffer with 1 mM DTT, followed by Western blot analysis using an anti-Bak antibody. Monomeric and oligomeric Bak are shown by open and closed arrowheads, respectively.

(C) Requirement of Bak for H1.2-induced cytochrome c release. Mitochondria were isolated from the livers of Bak-deficient mice ($^{-/-}$) and control littermates ($^{+/+}$) and were incubated with rH1.2 at the indicated concentrations. "Total" represents the total amount of cytochrome c in the same amount of mitochondria.

(D) Inhibition of histone H1.2-induced cytochrome c release by rBcl-xL. Rat liver mitochondria were incubated with rBcl-xL (30 μg/ml) or mock protein. After 5 min, 20 μM $CaCl_2$ or calf thymus histone H1 was added at the indicated concentrations and incubated for 25 min before cytochrome c release was tested.

Cytoplasmic Increase of Histone H1 Occurs Upstream of Apaf-1

To investigate whether the cytoplasmic increase of histone H1 occurred upstream or downstream of caspase-9/caspase-3 activation, Apaf-1-deficient MEFs, which lack activation of both caspases, were examined (Cecconi et al., 1998; Yoshida et al., 1998; also see Supplemental Figure S1A online at http://www.cell.com/cgi/content/full/114/6/673/DC1). Since MEFs are known to be resistant to DNA damage-induced apoptosis, the cells were transformed with E1A/Ras oncogenes to increase their apoptotic sensitivity (Lowe et al., 1993b). Both X-ray irradiated Apaf-1$^{+/+}$ and $^{-/-}$ MEFs showed a cytosolic increase of histone H1 as well as associated cytochrome c release as assessed by the biochemical and immunostaining methods (Supplemental Figures S1B–S1D). All these results indicated that the cytoplasmic increase of histone H1 occurred upstream of caspase-9/caspase-3 activation.

Release of Histone H1.2 from the Nucleus during X-Ray-Induced Apoptosis

The cytoplasmic increase of histone H1.2 during X-ray-induced apoptosis can be explained in two ways: either H1.2 is released from the nucleus, or H1.2 production is increased and/or nuclear import is disturbed. To distinguish between these possibilities, we inhibited the nuclear export of proteins possessing the nuclear export signal with leptomycin B (Fukuda et al., 1997). As shown in Figure 5A, leptomycin B caused concentration-dependent inhibition of the X-ray-induced cytoplasmic increase of H1 in MCF7 cells (a human breast carcinoma cell line possessing a functional p53 gene), indicating that H1 was released from the nucleus during X-ray-induced apoptosis. Expectedly, leptomycin B significantly inhibited X-ray-induced apoptosis in MCF7 cells (Figure 5B). Consistent with this concept, when Cy3-labeled recombinant H1.2 was microinjected into the cytoplasm of MCF7 cells, almost all of the H1.2 was

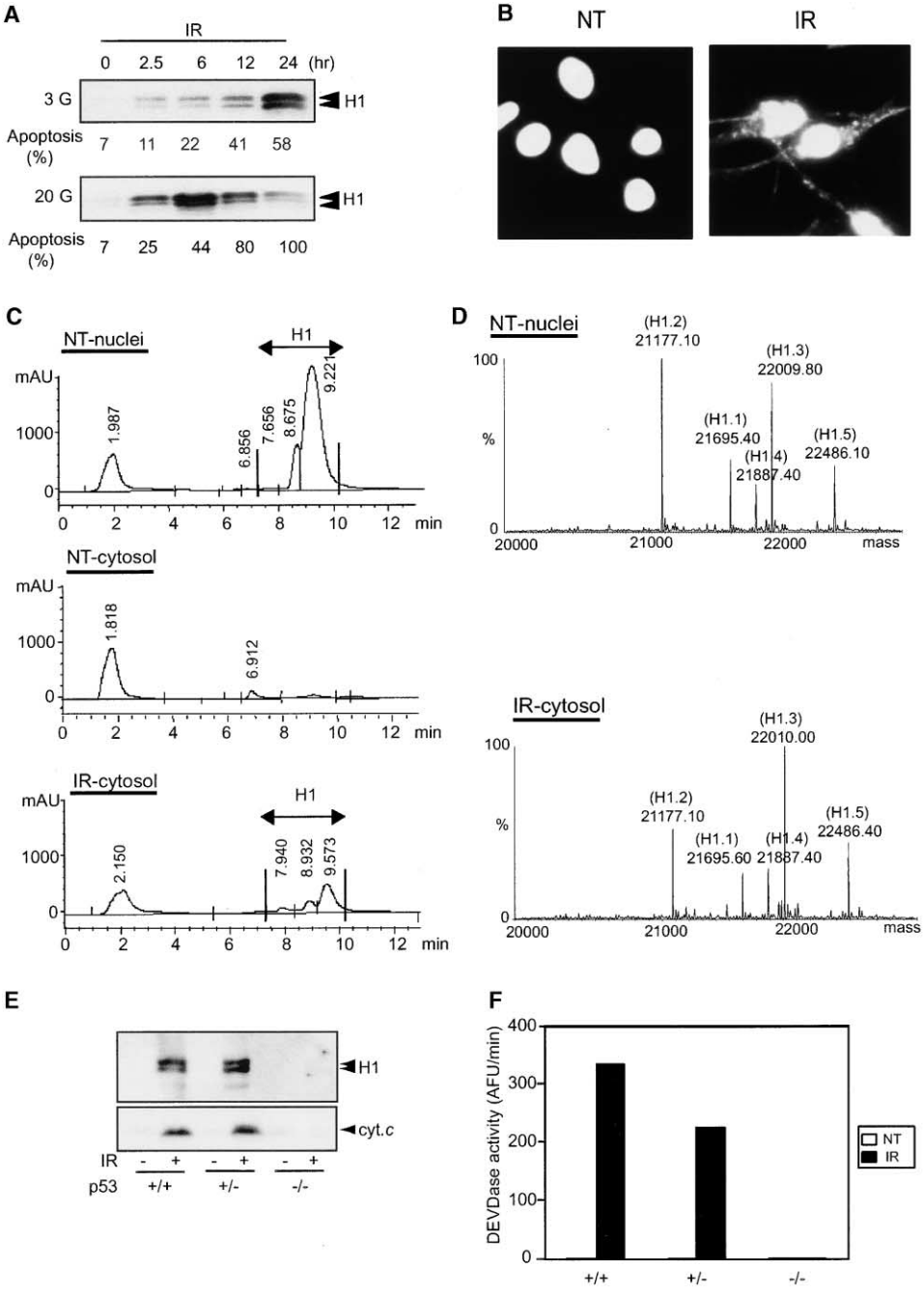

Figure 4. Cytoplasmic Accumulation of Histone H1.2 after X-Ray Irradiation and Its p53 Dependence

(A and B) X-ray-induced accumulation of histone H1.2 in the cytoplasm. (A) Thymocytes from healthy mouse were exposed to X-rays (3 and 20 Gy). At the indicated time, the extent of apoptosis was measured by annexin-V staining, and the cytoplasmic fractions were recovered. Then, samples (10 μg) were subjected to Western blot analysis for detection of histone H1. (B) E1A/ras-transformed MEFs were exposed to X-ray irradiation (20 Gy). After 24 hr, the cells were fixed and immunostained with an anti-histone H1 monoclonal antibody.

(C and D) HPLC and ESI-MS analysis of histone H1. Cytosolic and nuclear fractions were obtained from normal mouse thymus (NT) and from the thymus of a mouse 3 hr after X-ray irradiation (20 Gy) (IR). Histone H1 was purified from these fractions by acid extraction and was separated by RP-HPLC (C). The fractions indicated by H1 were collected and analyzed by ESI-MS (D). The highest peak was adjusted at 100%. The observed mass of each H1 subtype was almost equal to the calculated mass (see Figure 2D, table).

(E and F) p53-dependent increase of cytoplasmic histone H1.2 after X-ray irradiation. $p53^{+/+}$, $^{+/-}$, and $^{-/-}$ mice were exposed to 20 Gy of irradiation (IR [+]). After 6 hr, the thymi were excised, and cytosolic fractions were collected. Cytosolic fractions were also obtained from nonirradiated mice. Aliquots (30 μg) were subjected to Western blot analysis for detection of histone H1 and cytochrome c (E). Thymi were also lysed in isotonic buffer, and DEVDase activity was measured as described in Experimental Procedures (F).

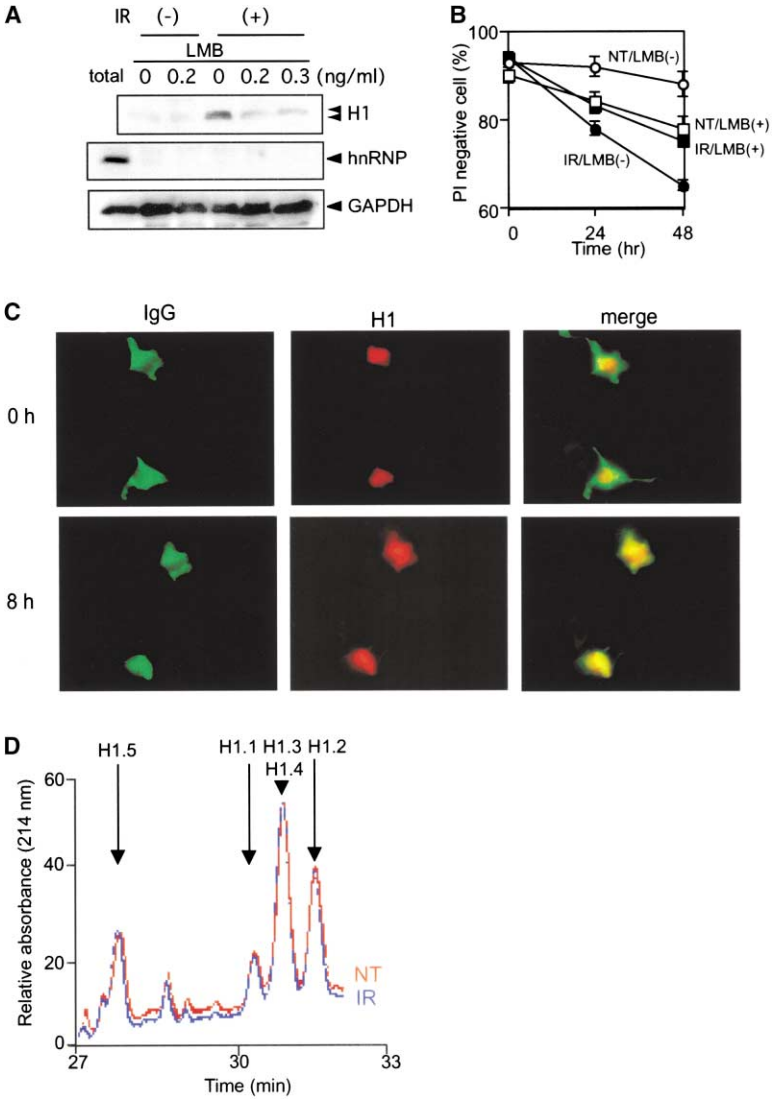

Figure 5. Release of Histone H1.2 from the Nucleus into the Cytoplasm by X-Ray Irradiation

(A and B) Inhibition of the X-ray-induced increase of cytosolic histone H1 and apoptosis by leptomycin B. (A) The indicated concentrations of leptomycin B were added to MCF7 cells 30 min before X-ray irradiation (30 Gy). After 24 hr, the cytoplasmic fractions were recovered and subjected to Western blot analysis for detection of histone H1. Samples were also subjected to Western blot analysis for detection of hnRNP and GAPDH as indicators of the nuclear and cytosolic fractions, respectively. (B) MCF7 cells were transiently transfected with caspase-3 cDNA (0.25 μg) for 24 hr together with DNA for GFP (0.05 μg). Then, the cells were exposed to 20 Gy of irradiation (IR) or were not irradiated (NT) in the absence (−) or presence (+) of 0.2 ng/ml leptomycin B. At the indicated times after irradiation, the cells were stained with propidium iodide to detect apoptosis among GFP-positive cells.

(C) Release of injected histone H1.2 after X-ray irradiation. Cy3-labeled histone H1.2 (8 mg/ml) was microinjected into the cytoplasm of MCF7 cells together with Alexa-488-labeled mouse IgG (see Supplemental Experimental Procedures). Then, the cells were exposed to irradiation (30 Gy), and the localization of histone H1.2 and IgG was assessed at the indicated time by fluorescence microscopy. Most of the histone H1.2 entered the nucleus rapidly after microinjection (0 hr), while a significant amount of microinjected histone H1.2 was also found in the cytoplasm after irradiation.

(D) No increase of histone H1 after X-ray irradiation. Histone H1 was isolated by acid extraction from the thymus of a healthy mouse (NT) and from the thymus of a mouse 3 hr after irradiation with 20 Gy (IR), and was analyzed by RP-HPLC.

rapidly transferred to the nucleus, and X-ray irradiation caused its partial release into the cytoplasm (Figure 5C). These results indicated that the X-ray-induced cytoplasmic increase of histone H1 was due to its release from the nucleus and was not related to new synthesis in the cytoplasm. It was also suggested that the nuclear import of histone H1 was impaired by X-ray irradiation.

Many genes, including *noxa* (Oda et al., 2000a), *puma* (Yu et al., 2001; Nakano and Vousden, 2001), and *bax* (Miyashita and Reed, 1995), are known to be upregulated during X-ray-induced apoptosis. As shown in Figure 5D, however, the total histone H1 content remained unchanged in mouse thymus after X-ray irradiation.

Inhibition of X-Ray-Induced Apoptosis by Reducing H1.2 Expression

As described above, histone H1.2 showed cytochrome c-releasing activity in a mitochondrial system, and the H1.2 level was increased in the cytoplasm by X-ray irradiation. Thus, H1.2 seemed to play an important role in the transduction of genotoxic stress signals from the nucleus to the mitochondria. To examine the role of H1.2 in X-ray irradiation-induced apoptosis, the level of this histone was reduced in MCF7 cells by the expression of H1.2 antisense RNA. Mouse histone H1.2 is analogous to human histone H1.2. By stably transfecting MCF7 cells with plasmid DNA expressing H1.2 antisense RNA, we isolated two clones (AS#1 and AS#2) with almost complete absence of histone H1.2, but not the other H1 subtypes (Figure 6A). The growth rate of AS#1 and AS#2 cells was similar to that of the parent cells and of several vector-transfected clones (vec#1, vec#2, and vec#3; data not shown). When these cells were irradiated and cytosolic fractions (free of mitochondria) were analyzed, apoptotic release of cytochrome c was observed in vector DNA-transfected, but not in antisense DNA-transfected, cells (Figure 6B). Immunostaining also revealed that cytochrome c was released from the mitochondria in half of the irradiated vec#1 and vec#2 cells after 24 hr, whereas it was still located in the mitochondria of the majority of AS#1 and AS#2 cells (Figure 6C and data not shown), indicating that histone H1.2 was required for the X-ray-induced release of cytochrome c.

Since histone H1.2 expression could influence the

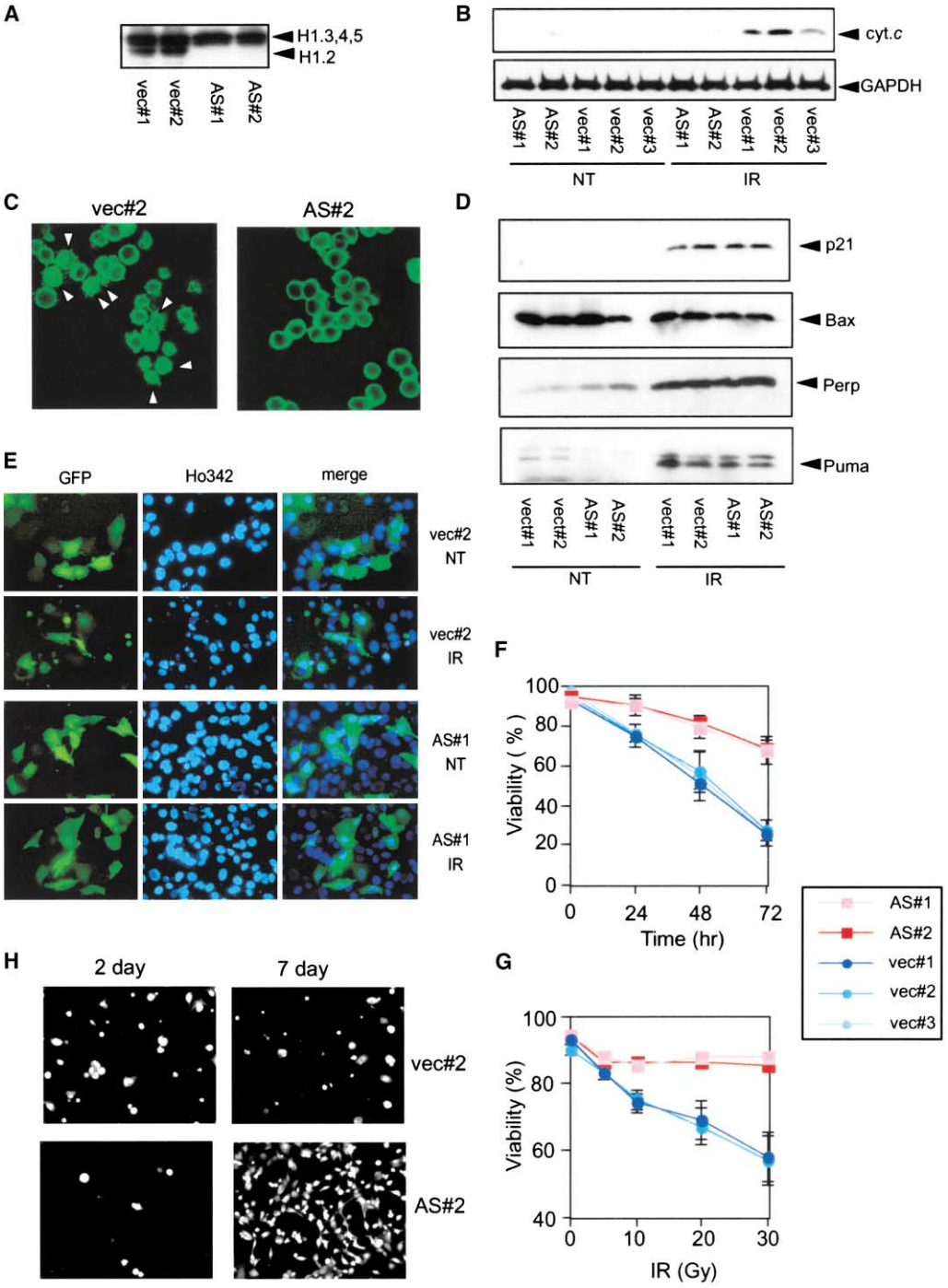

Figure 6. Inhibition of X-Ray-Induced Apoptosis by Reducing Histone H1.2 Expression

(A) Reduction of histone H1.2 by antisense RNA. MCF7 cells were stably transfected with the plasmid for histone H1.2 antisense RNA (AS) or with the empty vector (vec). Cell lysates were subjected to Western blot analysis using anti-histone H1 antibody.

(B and C) Prevention of X-ray-induced cytochrome c release by reduction of histone H1.2. The indicated MCF7 variants were exposed to irradiation (30 Gy) (IR) or were not treated (NT). (B) After 24 hr, cytosolic fractions were collected and aliquots of the fractions were subjected to Western blot analysis for detection of cytochrome c and of GAPDH as a loading control. (C) At 24 hr after irradiation, cells were fixed and immunostained with anti-cytochrome c antibody. Representative cells showing cytochrome c release are indicated by arrowheads.

(D) Unchanged expression of p21, Bax, Perp, and Puma after reduction of histone H1.2. MCF7 variants were exposed to irradiation (30 Gy) (IR) or were not treated (NT). After 24 hr, cells were lysed in RIPA buffer, followed by Western blot analysis for p21, Bax, Perp, and Puma.

(E–G) Inhibition of X-ray-induced apoptosis by reduction of histone H1.2. (E and F) MCF7 variants were transiently transfected with caspase-3 DNA plus GFP DNA for 48 hr. Then, the cells were exposed to irradiation (20 Gy) (IR) or were not treated (NT). After 24 hr, the cells were stained with Hoechst 33342 (Ho342), and apoptotic cells were detected by examining the nuclear morphology. Representative photographs are shown in (E). Viability at the indicated times after X-ray irradiation was calculated as the number of apoptotic cells relative to GFP-positive cells (F). Data are expressed as the mean ± SD for four independent experiments. (G) The same experiment as shown in (F) was performed using the indicated doses of irradiation. Cell death was assessed at 24 hr.

(H) Increased cell proliferation after X-ray irradiation due to reduction of histone H1.2. MCF7 variants were exposed to irradiation (20 Gy). After 2 days, the cells were collected, and 1000 cells were reseeded onto 6-well dishes. At the indicated times after irradiation, cells were stained with 10 μM calcein-AM, an indicator of viability, and observed under a fluorescence microscope.

transcription of certain genes (Vignali and Workman, 1998), and since X-ray-induced apoptosis is at least partly controlled by a p53-dependent increase of pro-apoptotic molecules (such as Bax, Perp, Noxa, p53AIP1, and Puma), the difference in apoptotic cytochrome c release between vec#1, vec#2 and AS#1, AS#2 cells might be due to a difference of p53-dependent transcription. Therefore, we examined the expression of some p53-regulated molecules and found that the expression of p21, Bax, Perp, and Puma did not differ between vec and AS cells (Figure 6D).

The requirement for histone H1.2 for X-ray-induced apoptosis was also assessed from the aspect of cell viability. Since MCF7 cells did not show typical apoptotic features due to the lack of caspase-3, MCF7 derivatives were transiently transfected with caspase-3 DNA and GFP DNA (to identify transfected cells) and then irradiated. Apoptosis was estimated from the nuclear morphology after staining with Hoechst 33342. The caspase-3-transfected vec#1 and #2 cells became apoptotic with nuclear and cellular shrinkage only after irradiation in a time- and dose-dependent manner (Figures 6E–6G). In contrast, a smaller number of caspase-3-transfected AS#1 and AS#2 cells died after irradiation (Figures 6E–6G). A similar result was obtained when apoptosis was assessed by annexin-V staining of GFP-positive cells (data not shown). To confirm the superior viability of AS cells after X-ray irradiation, AS#2 and vec#2 cells were irradiated without DNA transfection, harvested, and cultured for 2 days. As can be seen in Figure 6H, AS#2 cells had much greater proliferative activity than vec#2 cells, indicating that AS cells actually survived despite X-ray irradiation. We also found that transfection of AS#1 cells with H1.2 DNA, but not H1.3, H1.4, or H1.5 DNA, restored their sensitivity to irradiation (Supplemental Figure S2). Consistent with these results, X-ray-induced apoptosis was reduced when H1 was inhibited by microinjection of anti-histone H1 antibodies (Supplemental Figure S3). All these results indicated that histone H1.2 plays an important role in X-ray-induced apoptosis.

Specific Role of Histone H1.2 in Apoptosis Induced by DNA Double-Strand Breaks

Next, we examined the role of histone H1.2 in other forms of apoptosis using the vec and AS clones of MCF7 cells. When these cells were exposed to UV (254 nm) irradiation, both vec (#1, #2, and #3) and AS (#1 and #2) cells exhibited similar levels of release of cytochrome c as well as the induction of apoptosis (Figures 7A–7C). Similarly, AS#1 and AS#2 cells did not show increased resistance against paclitaxel and TNF-α compared with control vec#1, vec#2, and vec#3 cells (Figure 7C). However, AS#1 and AS#2 cells were more resistant to etoposide than vec#1, vec#2, or vec#3 cells (Figure 7C). These results indicated that histone H1.2 is specifically required for apoptosis induced by etoposide and X-rays, both of which cause DNA double-strand breaks. Since histone H1.2 was involved in X-ray-/etoposide-induced apoptosis, which is p53-dependent, and since release of H1.2 is also dependent on p53, we examined the involvement of histone H1.2 in p53-induced apoptosis. Transfection with p53 DNA induced apoptosis equally in both AS#2 and vec#2 cells (Figure 7D), and a cytosolic increase of histone H1 was not observed in p53-transfected vec#2 cells (Figure 7E). These results indicated that histone H1.2 was not involved in p53-induced apoptosis. The involvement of H1.2 in apoptosis induced by DNA double-strand breaks, but not other stimuli, was confirmed by silencing H1.2 using siRNA (Figures 7F–7H and Supplemental Figure S4).

Histone H1.2-Deficient Mice Show Cellular Resistance to X-Ray-Induced Apoptosis

Finally, we examined mice lacking histone H1.2. These mice do not show any phenotypic abnormalities (Fan et al., 2001). Thymocytes isolated from H1.2 knockout (KO) and wild-type (wt) mice (Figure 8A) showed no differences of their CD4/8 profile (data not shown). When the thymocytes were X-ray irradiated, H1.2-KO thymocytes showed superior viability to wt thymocytes over a wide range of radiation doses (Figures 8B and 8C). Consistent with the results obtained using antisense RNA and siRNA (Figures 7C, 7G, and 7H), etoposide-induced apoptosis, but not staurosporine-induced apoptosis, was less prominent in H1.2 KO thymocytes than in wt thymocytes (Figures 8D and 8E). The reason that eliminating H1.2 has only a partial effect on X-ray-induced apoptosis might have been due to activation of the Bax pathway, which is nonessential in the presence of histone H1.2 (Figure 1C). Alternatively, it could be that other H1 subtypes can partially substitute for H1.2 in this role in H1.2 KO mice. We also examined the involvement of histone H1.2 in X-ray-induced apoptosis of small bowel cells, a site where the contribution of the Bax has been reported to be very limited (Pritchard et al., 1999). When wt mice were exposed to X-ray irradiation (10 Gy) and sacrificed after 2 days, the small intestine was severely damaged, with denudation of the crypt and villus system (Figure 8F), as well as positive TUNEL-staining of a large number of epithelial cells and enterocytes (Figure 8F). In contrast, the small bowel looked normal after X-ray irradiation of H1.2 KO mice, and only a few TUNEL-positive cells were observed in the columnar epithelium (Figure 8f), indicating that X-ray-induced apoptosis was strongly inhibited by H1.2 deficiency. Consistently, apoptosis-associated cleavage of lamin B1 and ICAD, as well as activation of caspase-3, were observed in the small intestine of WT mice, but not in H1.2 KO mice (Figure 8G), confirming the essential role of H1.2 in X-ray-induced apoptosis.

Discussion

Various apoptotic stimuli, including X-ray irradiation, Ca^{2+} overload, and growth factor deprivation, initially activate individual stimulus-specific signaling pathways, which subsequently converge into a common pathway at the mitochondria. As molecules that play a role in transmitting DNA damage-induced apoptotic signals, a variety of proteins have been described including Bax (Miyashita and Reed, 1995), PIGs (Polyak et al., 1997), Noxa (Oda et al., 2000a), Puma (Nakano and Vousden, 2001), Perp (Attardi et al., 2000), nuclear orphan receptor TR3 (Li et al., 2000), p53 (Marchenko et al., 2000), and p53AIP (Oda et al., 2000b). Among

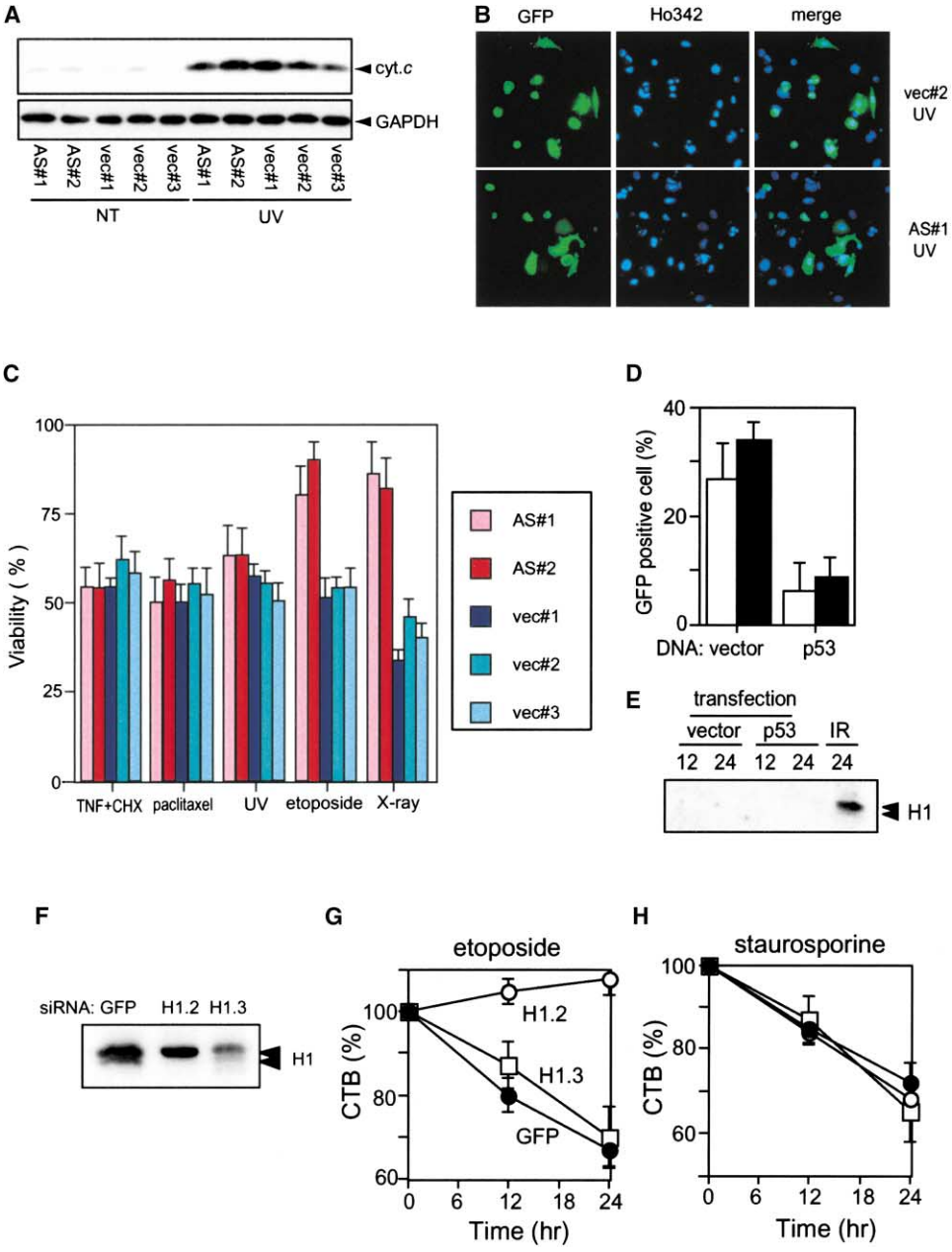

Figure 7. Requirement of Histone H1.2 for Apoptosis Induced by DNA Double-Strand Breaks, but Not Other Stimuli

(A) No effect of reduction of histone H1.2 on UV-induced cytochrome c release. The indicated MCF7 variants were exposed to UV (254 nm) irradiation (100 J/m^2) (UV) or were not treated (NT). After 24 hr, cytosolic fractions were collected and subjected to Western blot analysis for detection of cytochrome c and GAPDH (as a loading control).

(B) No effect of reduction of histone H1.2 on UV-induced apoptosis. The indicated MCF7 variants were transiently transfected with caspase-3 cDNA, together with GFP DNA, for 48 hr. Then, the cells were exposed to UV irradiation (100 J/m^2). After 24 hr, the cells were stained with Hoechst 33342, and the nuclear morphology was observed under a fluorescence microscope.

(C) Effect of reduction of histone H1.2 on various forms of apoptosis. The indicated MCF7 variants were transiently transfected with caspase-3 cDNA, together with GFP DNA, for 24 hr. Then, the cells were incubated with TNF-α (10 ng/ml) and cycloheximide (CHX) (1 μg/ml), paclitaxel (10 nM), UV (100 J/m^2), etoposide (100 μM), or X-ray irradiation (30 Gy) for 24 hr. Apoptosis was assessed as in (B). Data are expressed as the mean $\pm$ SD for three independent experiments.

(D) No effect of a decrease of histone H1.2 on p53-induced apoptosis. MCF7 vec#2 cells (open column) and AS#2 cells (solid column) were transiently transfected with p53 cDNA (1 μg) plus GFP DNA (0.2 μg) for 24 hr. Then GFP-positive cells were detected by flow cytometry. Data are expressed as the mean $\pm$ SD for three independent experiments.

(E) No release of histone H1.2 after transfection with p53. MCF7 vec#2 cells were transiently transfected with p53 cDNA or vector (1 μg) or were subjected to X-ray irradiation (IR). At the indicated times, cytoplasmic fractions were collected and subjected to Western blot analysis for detection of histone H1.

(F–H) Inhibition of etoposide-induced, but not staurosporine-induced, apoptosis by silencing of histone H1.2 with siRNA. HCT116 cells were transfected with histone H1.2 siRNA (open circles), histone H1.3 siRNA (squares), or GFP siRNA (closed circles) as a control, as described in Experimental Procedures. After 24 hr, a quarter of the cells were lysed, followed by Western blot analysis using anti-histone H1 antibody (F). The remaining cells were treated with 100 μM etoposide (G) or 1 μM staurosporine (H). Cell death was assessed by the CTB assay at the indicated times. Data are expressed as the mean $\pm$ SD for four independent experiments.

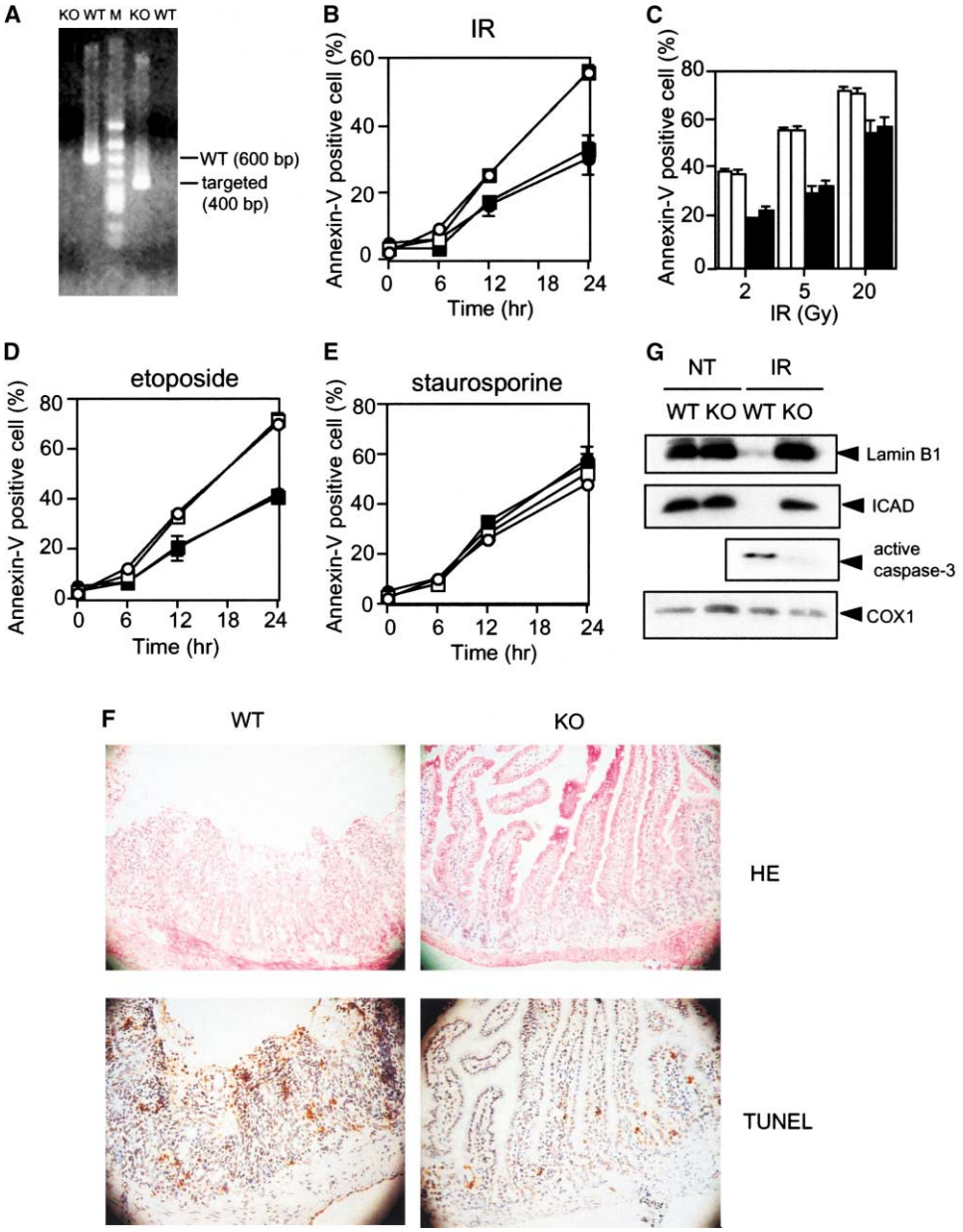

Figure 8. Inhibition of X-Ray- and Etoposide-Induced Apoptosis by Histone H1.2 Deficiency

(A) Genotypic analysis of histone H1.2-deficient mice. PCR of mouse tail DNA was performed. The two left lanes and two right lanes show PCR-amplified DNA using primers for the wild-type and targeted alleles, respectively. Bands of 600 and 400 bp represent the wild-type and targeted alleles, respectively. "M" indicates the DNA size marker (pSKMBKR2R/Dpn I).

(B–E) Inhibition of X-ray-induced and etoposide-induced thymocyte apoptosis by histone H1.2 deficiency. Thymocytes isolated from wild-type mice (open symbols) and H1.2 knockout mice (closed symbols) were treated with 5 Gy (B) or the indicated doses of X-ray irradiation (C), 10 μM etoposide (D), or 0.5 μM staurosporine (E). At the indicated times (B, D, and E), or at 24 hr (C), apoptosis was assessed by annexin-V staining.

(F and G) Inhibition of X-ray-induced apoptosis in the small bowel by histone H1.2 deficiency. Wild-type mice (WT) and H1.2 knockout mice (KO) were irradiated with X-rays (10 Gy). (F) After 48 hr, equivalent segments of the jejunum were excised and subjected to hematoxylin and eosin (HE) and TUNEL staining. Specimens were observed under a light microscope (×200). (G) Other equivalent segments (from adjacent to the duodenum) were excised and homogenized. The homogenate was subjected to Western blot analysis with anti-lamin B1, anti-ICAD, anti-active caspase-3, and anti-COX1 antibodies.

these proteins, Bax, Noxa, Puma, TR3, p53, and p53AIP have been implicated in direct signaling to the mitochondria. Because DNA damage-induced apoptosis depends on the transcription factor p53 in many types of cells, many candidates for DNA damage-induced apoptotic signaling molecules (e.g., Noxa, Puma, Perp, and p53AIP) have been identified on the basis of transcriptional activation by p53. Some of these proteins indeed play a role in DNA damage-induced apoptosis because reduced expression of their genes results in only partial

resistance to DNA damage. Such findings suggest that these candidate proteins function cooperatively or that a crucial signaling molecule is still undiscovered. In this context, it is interesting to note that deficiency of p53 or both of its relatives, p63 and p73, results in complete resistance to doxorubicin-induced apoptosis and prevents the expression of p53-activated genes such as *bax* and *perp* in MEFs, indicating that transcriptional activation of these genes not only requires p53, but also p63 or p73 (Flores et al., 2002). In p63- or p73-deficient MEFs, apoptosis was slightly reduced, whereas transcriptional activation of Bax, Noxa, and Perp was comparable to that in $p63^{+}/p73^{+}$ MEFs (Flores et al., 2002). Furthermore, it has been reported that MEFs lacking IRF-1 are resistant to DNA damage-induced apoptosis, whereas the target genes of p53, including *bax* and *noxa*, are normally activated (Tanaka et al., 1996; Oda et al., 2000a). These results suggest that the genes activated by p53 may not be sufficient to cause DNA damage-induced apoptosis in MEFs.

We adopted a biochemical approach to investigate the transmission of X-ray-induced apoptotic signals to the mitochondria in thymocytes by searching for a molecule that appeared in the cytoplasm after irradiation and that could induce cytochrome c release from isolated mitochondria. As a result, we identified histone H1.2, which is a subtype of linker histone H1. We showed that histone H1.2 is not only involved in apoptosis induced by X-rays, but also in apoptosis induced by etoposide (an inhibitor of topoisomerase II); both of these stimuli cause DNA damage that primarily involves double-strand breaks. In contrast, H1.2 was not related to other forms of apoptosis induced by TNF-α/cycloheximide, staurosporine, and paclitaxel. It was particularly interesting that histone H1.2 did not play an important role in apoptosis induced by UV irradiation, which also causes DNA damage that primarily involves base modifications. UV irradiation might also activate pathways other than the DNA damage-related pathway to induce apoptosis (Rosette and Karin, 1996). It should be noted that DNA double-strand breaks, but probably not UV damage, trigger a megabase range of chromatin remodeling (Rogakou et al., 1999), which leads to release of a significant amount of H1 from the chromatin. Thus, histone H1.2 seems to be specifically involved in apoptosis induced by DNA double-strand breaks.

After X-ray irradiation, histone H1.2 accumulated in the cytoplasm in a p53-dependent manner. Using leptomycin B (an inhibitor of nuclear export) and by microinjecting Cy3-labeled histone H1 into cells, we showed that cytoplasmic accumulation of histone H1.2 after X-ray irradiation was mainly mediated by its release from the nucleus. The form of histone H1.2 released from the nucleus during X-ray-induced apoptosis seemed to be chemically identical to the nuclear form of this histone. Since H1.2 is normally bound to chromatin in the nucleus (Vignali and Workman, 1998), DNA double-strand breaks or the subsequent p53-dependent repair process may cause its release into the nucleoplasm and subsequently into the cytoplasm. The amount of histone H1.2 released from the chromatin might be used for monitoring the extent of DNA damage. The X-ray irradiation-dependent release of nuclear histone H1 and its accumulation in the cytoplasm suggest that the nuclear import/export machinery must be affected by X-ray-irradiation, although the precise mechanisms involved are still to be determined.

It was reported that a fraction of phosphorylated histone H1 is found in the cytoplasm at M phase, whereas the rest of phosphorylated H1 and all nonphosphorylated H1 remain bound to chromatin (Bleher and Martin, 1999). This suggests that the amount of cytoplasmic phosphorylated H1 at M phase might not be sufficient for damaging the mitochondria. Alternatively, phosphorylated H1.2 might not have cytochrome c-releasing activity. In fact, we could only detect histone H1 in the cytoplasm of M phase cells at a much lower level than that of X-ray-irradiated cells and also found that cytosolic histone H1 isolated from M phase cells shows a significantly weaker cytochrome c-releasing activity (our unpublished data).

As a candidate signaling molecule for X-ray-induced apoptosis, histone H1.2 shows some different properties from previously described molecules. First, most of the candidate X-ray-induced apoptotic signaling molecules are only present at low levels in living cells and show transcriptional activation by X-ray irradiation, whereas a change in the subcellular location of histone H1.2 is the crucial event. Second, many of the proposed signaling molecules, such as Noxa or Puma (BH3-only members) and Bax (a multidomain member), belong to the Bcl-2 family, whereas histone H1.2 possesses neither a BH3 domain nor any other significant homology with Bcl-2. Since multidomain proapoptotic members of the Bcl-2 family like Bax and Bak act as a gateway for a variety of apoptotic signals (Lindsten et al., 2000, Wei et al., 2001), including X-ray-induced DNA damage, Noxa, Puma, and Bax probably induce mitochondrial membrane permeabilization through interaction with Bcl-2 family members. How, then, does H1.2 induce cytochrome c release? Histone H1.2 did not show any direct interaction with Bcl-2 family members (our unpublished data). Several molecules other than Bcl-2 family members, such as TR3 (Li et al., 2000), p53AIP1 (Oda et al., 2000b), and PKC (Majumder et al., 2000), have been shown to directly signal the mitochondria by a still-unknown mechanism. Although it has not been determined how histone H1.2 induces cytochrome c release, we showed that histone H1.2-induced cytochrome c release was dependent on multidomain proapoptotic Bcl-2 family members and that histone H1.2 caused activation of Bak, as assessed using an anti-Bak antibody specific for activated Bak and a protein crosslinker to detect oligomerization. Since one of the BH3-only proteins, tBid, has been shown to have the lipid-transfer activity (Esposti et al., 2001) and the ability to disrupt lipid membranes (Epand et al., 2002) and since mitochondrial damage has been shown to activate Bax (Yamaguchi and Wang, 2002), histone H1.2 might affect lipid membranes and indirectly activate multidomain proapoptotic Bcl-2 family members, leading to permeabilization of the outer mitochondrial membrane. Approximately 30% of histone H1.2 is composed of cationic amino acid residues, many of which are located in the α-helix (Pepe et al., 1990; Vila et al., 2000). Some of these α-helical regions might function like natural antibiotic peptides, such as KLAKLAKKLAKLAK, which forms an α-helix with cationic residues on one side, thereby inter-

acting with anionic phospholipids to disrupt negatively charged membranes, leading to apoptosis (Ellerby et al., 1999). Further studies are necessary to identify the domain of histone H1.2 that is essential for its cytochrome c-releasing activity.

Humans and mice have eight histone H1 genes. Among them, all of the somatic H1s (H1.1–H1.5) are ubiquitously expressed in all body tissues throughout development (Franke et al., 1998). Histone H1.2 has a high metabolic stability (Franke et al., 1998). As shown here, although all histone H1s are similar to each other, only histone H1.2 has the strong ability to induce mitochondrial membrane permeabilization. The major difference between histone H1.2 and other H1s is found at the C-terminal region, since the KXXKP sequence exists in all H1s except for H1.2. This sequence might negate the proapoptotic activity of histone H1s other than H1.2.

In conclusion, we showed that during DNA double-strand break-induced apoptosis, the linker histone H1.2 is released from the nucleus into the cytoplasm where it triggers permeabilization of the outer mitochondrial membrane. We propose that histone H1.2 probably cooperates with various proapoptotic proteins, including some targets of p53.

Experimental Procedures

Information on reagents, amino acid sequencing, production of recombinant proteins, HPLC/MS, and microinjection can be found online in the Supplemental Experimental Procedures section.

Measurement of Mitochondrial Biochemical Parameters

Livers harvested from male Donryu rats were homogenized with a glass-Teflon Potter homogenizer. Mitochondria were isolated in 0.3 M mannitol, 10 mM potassium-Hepes (pH 7.4), 0.2 mM EDTA, and 0.1% fatty acid-free BSA, as described previously (Shimizu et al., 1998). The mitochondria were washed twice and resuspended in the same medium without EDTA (MT-1medium). Mitochondria were also prepared from the livers of Bak knockout mice and their normal littermates.

Isolated mitochondria (1 mg/ml protein) were incubated with the indicated proteins at 25°C in MT-1 medium plus 100 μM potassium phosphate (pH 7.4) and 4.2 mM succinate (MT-2 medium), after which $\Delta\psi$ and cytochrome c release were measured. $\Delta\psi$ was assessed by measuring the $\Delta\psi$-dependent uptake of rhodamine 123 using a spectrophotometer (Hitachi F-4500), as described elsewhere (Shimizu et al., 1998). For detection of cytochrome c release after a 30 min incubation, mitochondria (100 μg protein) were centrifuged at 12,000 × g for 5 min, and aliquots of the supernatants were subjected to Western blot analysis using an anti-cytochrome c antibody.

Preparation of the Cytosolic Fraction and Total Cell Lysate

Male Donryu rats or p53-deficient mice and their normal littermates were exposed to X-ray irradiation (20 Gy at a rate of 1.76 Gy/min; Radioflex 350, RIGAKU). The thymus was then excised from each animal and homogenized in 5 volumes of isotonic buffer (20 mM potassium-Hepes [pH 7.4], 10 mM KCl, 1.5 mM $MgCl_2$, 250 mM sucrose, 1 mM Na^{2+}-EDTA, 1 mM DTT, and 0.1 μM PMSF) by 15 strokes of a glass-Teflon Potter homogenizer. The homogenate was centrifuged at 100,000 × g for 1 hr, and the supernatant was collected as the cytosolic fraction. Control cytosol was also obtained from healthy animals in the same way.

For the detection of released cytochrome c, the cytosolic fraction was collected from MEFs and MCF7 cells after incubation with 0.3 mg/ml digitonin for 5 min at 37°C in isotonic buffer. The cells were centrifuged at 12,000 × g for 5 min, and the supernatants (which mainly contained the cytosol but not the organelles) were subjected to Western blot analysis.

For the detection of extranuclear histone H1, thymocytes, E1A/Ras-transformed MEFs, and MCF7 cells were suspended in the hypotonic buffer (100 mM Na^{2+}-Hepes [pH 9.4], 1.5 mM $MgCl_2$, 10 mM KCl, and 0.5 mM 2-mercaptoethanol) for 10 min. Cells were lysed with 0.2% NP-40 for 3 s with vortexing and centrifuged at 7500 × g for 10 min. The supernatant (which contained cytosol and organelles, but not nuclei) was subjected to Western blot analysis. In some experiments, cells were lysed by RIPA buffer (50 mM Tris-HCl [pH 8.0], 20 mM EDTA, 1% SDS, and 100 mM NaCl).

Purification of Histone H1.2 As a Cytochrome c-Releasing Factor and Total Histone H1

All purification steps were carried out at 4°C. The cytosolic fraction of the thymus was collected from X-ray irradiated rats, as described above and then was applied to a Poros HQ column (4.6 × 100 mm; Applied Biosystems) equilibrated with buffer A (20 mM potassium-Hepes [pH 7.4], 10 mM KCl, 1.5 mM $MgCl_2$, 1 mM Na^{2+}-EDTA, and 1 mM DTT). The column was washed with three column volumes of buffer A and was eluted with 65 ml of a linear NaCl gradient (0–0.75 M). Two fractions (A, 0.25 M; B, 0.45 M) were found to show cytochrome c-releasing activity. Fraction B (9 ml) was concentrated with a Microcon centrifugal filter (MWCO 5 kDa; Millipore), loaded onto a Superdex-200 HR column (10/30; Pharmacia) (24 ml) equilibrated with buffer A containing 0.1 M NaCl, and sieved with the same buffer. The active fraction (1.5 ml) obtained from the gel filtration column was loaded onto a Mini S PC 3.2/3 column (0.24 ml) equilibrated with buffer A containing 0.1 M NaCl, washed with buffer A containing 0.25 M NaCl and eluted with 3.4 ml of a linear NaCl gradient (0.25–1 M). Fractions (100 μl) were collected and assayed for cytochrome c-releasing activity.

We also used a Poros HS column (4.6 × 100 mm; Applied Biosystems) equilibrated with buffer A after the Poros HQ column instead of the Superdex 200 and Mini S columns. Elution was carried out using 15 ml of a linear NaCl gradient (0–1 M).

To purify mouse H1, nuclei were isolated from the thymi of healthy mice, and histone H1 was partially purified by the acid extraction method using 0.2 M sulfuric acid as described elsewhere (Kratzmeier et al., 1999). Then the extract was dialyzed against distilled water and was loaded onto a Poros HQ column followed by a Mini S column, as described above.

Assay of Bak Activation

HeLa cells were permeabilized for 3 min at 25°C with 30 μg/ml digitonin in isotonic buffer, and then incubated with the indicated proteins for 10 min at 25°C. Subsequently, the cells were fixed with paraformaldehyde and stained with an anti-active Bak antibody (Oncogene, Ab-1).

For detection of Bak oligomers, isolated mitochondria were incubated for 30 min with 10 mM BMH (an uncleavable protein cross-linker). Then the mitochondria were centrifuged at 15,000 × g for 3 min, dissolved in 2× sample buffer (0.2 M Tris-Cl [pH 6.8], 10% SDS-PAGE, 25% 2-mercaptoethanol, 25% glycerol, and 0.01% BPB) with 1 mM DTT, and boiled for 5 min to inactivate BMH. Oligomerized Bak was detected by Western blot analysis using an anti-Bak antibody.

Cell Lines

MEFs, MCF7 cells, and HCT116 cells, which all possess a functional p53 gene, were cultured at 37°C in DMEM containing 10% fetal bovine serum under an atmosphere of 10% CO_2. HeLa cells were maintained at 37°C in RPMI containing 10% fetal bovine serum under 10% CO_2. MEFs were transfected with E1A and ras, as described previously (Lowe et al., 1993b), in order to sensitize the cells to X-ray-induced apoptosis. Briefly, a retroviral PLPC vector carrying adenovirus 5 E1A and the puromycin-resistance gene or ras and the hygromycin phosphotransferase gene was used to transfect cells via the packaging cell line ψ2. MEFs were first transfected with E1A, and stable transfectants were selected by incubation with 2 μg/ml puromycin. Next, E1A-transformed MEFs were transfected with ras, and stable transfectants were selected by incubation with 200 μg/ml hygromycin.

To reduce the expression of histone H1.2, MCF7 cells were transfected with the pUC-CAGGS expression vector bearing human histone H1.2 cDNA with the reverse orientation.

siRNA

All the siRNAs were produced by Dharmacon Research. The sequences used were as follows (numbers in parentheses indicate nucleotide positions within the respective open reading frame): human histone H1.2-siRNA, 5′-AAGAGCGUAGCGGAGUUUCUC-3′ (155–175); human histone H1.3-siRNA, 5′-AAGAAGGCAGGCGCAACUGCU-3′ (73–93); and GFP-siRNA, 5′-GGCUACGUCCAGGAGCGCACC-3′ (274-294). Cells (1×10^6) were transfected three times on alternate days with 10 μg of siRNA using lipofectamine 2000.

Immunostaining of Endogenous Histone H1 and Cytochrome c

MEFs were washed with PBS and fixed in 4% formaldehyde on ice for 10 min. After washing three times, cells were permeabilized with 0.1% Triton X-100 in PBS at room temperature for 15 min and were incubated with 2% fetal bovine serum for 30 min. Then anti-histone H1 mAb (20 μg/ml) was added with 3% milk for 1 hr at room temperature. After washing another three times, the cells were incubated for 1 hr in the presence of a secondary antibody conjugated with Alexa-488 and were examined under a fluorescence microscope (IX70; Olympus). Localization of cytochrome c was also assessed by immunostaining using an anti-cytochrome c mAb.

Analysis of Cell Death

Cell viability was assessed by nuclear morphology after staining with Hoechst 33342, PI staining, annexin-V staining, the TUNEL assay, or the Cell Titer Blue (CTB) assay. Briefly, cells were stained with 1 μM PI, 1 μM Cy3-conjugated annexin-V, or 1 μM Hoechst 33342 for 5 min at room temperature and were analyzed with a flow cytometer (Becton-Dickinson, FACS Caliber) or under a fluorescence microscope (Olympus, BX50). The CTB assay, which measured the metabolic activity of viable cells, was carried out using Cell Titer Blue reagent according to the supplier's protocol. In some experiments, MCF7 cells were transiently transfected with caspase-3 cDNA (0.25 μg) for 48 hr using Effectene in order to sensitize the cells to X-ray-induced apoptosis, together with 0.05 μg of pEGFP-N1 DNA (Clontech), which was used to monitor DNA transfection. Then the transfected cells were treated to undergo apoptosis. After staining with 1 μM Hoechst 33342, the extent of apoptosis was calculated as the percentage of GFP-positive cells with nuclear fragmentation relative to all GFP-positive cells. DEVDase activity was measured as described elsewhere (Shimizu et al., 1996).

Analysis of Histone H1.2-Deficient Mice

H1.2-deficient mice that had been backcrossed to C57BL/6 over 10 generations were genotyped by PCR of tail DNA. The wild-type H1.2 allele was identified using sense (5′-CTGCCACACCCAAAAAGG-3′) and anti-sense (5′-GAGCATAGAAGCCACCTACAAG-3′) primers, and the mutant H1.2 allele was identified using a PGK-Hygro gene sense primer 5′-GCTGCTAAAGCGCATGCTCCA-3′ and the same anti-sense primer as that for the wild-type allele.

6-month-old H1.2-deficient mice and wild-type C57BL/6 mice were studied. Thymocytes (1×10^6) were plated into each well of 6-well dishes and were exposed to apoptotic stimuli. Then, the cells were stained with Cy3-labeled annexin-V. To assess the effect on the small intestine, mice were exposed to 10 Gy of X-ray irradiation. After 48 hr, equivalent segments of the small intestine (jejunum) were excised and frozen at −80°C in Tissue-Tek for HE and TUNEL staining. Other segments (from adjacent to the duodenum) were also excised and homogenized in PBS containing 2% CHAPS. Homogenates were subjected to Western blot analysis.

Acknowledgments

We are grateful to Dr. C.B. Thompson for providing $Bak^{-/-}$ mice. We also thank Dr. S.W. Lowe for providing E1A and Ras plasmids and Dr. X. Wang for Apaf-$1^{+/+}$ and $^{-/-}$ MEFs. This study was supported in part by a grant for Scientific Research on Priority Areas, a grant for Center of Excellence Research, a grant for Scientific Research from the Ministry of Education, Science, Sports, and Culture of Japan, and by Special Coordination Funds for Promoting Science and Technology from the Science and Technology Agency of Japan.

Received: March 10, 2003
Revised: August 13, 2003
Accepted: August 27, 2003
Published: September 18, 2003

References

Adams, J.M., and Cory, S. (1998). The Bcl-2 protein family: arbiters of cell survival. Science *281*, 1322–1326.

Albig, W., and Doenecke, D. (1997). The human histone gene cluster at the D6S105 locus. Hum. Genet. *101*, 284–294.

Antonsson, B., Montessuit, S., Lauper, S., Eskes, R., and Martinou, J.C. (2000). Bax oligomerization is required for channel-forming activity in liposomes and to trigger cytochrome *c* release from mitochondria. Biochem. J. *345*, 271–278.

Antonsson, B., Montessuit, S., Sanchez, B., and Martinou, J.C. (2001). Bax is present as a high molecular weight oligomer/complex in the mitochondrial membrane of apoptotic cells. J. Biol. Chem. *276*, 11615–11623.

Attardi, L.D., Reczek, E.E., Cosmas, C., Demicco, E.G., McCurrach, M.E., Lowe, S.W., and Jacks, T. (2000). PERP, an apoptosis-associated target of p53, is a novel member of the PMP-22/gas3 family. Genes Dev. *14*, 704–718.

Bleher, R., and Martin, R. (1999). Nucleo-cytoplasmic translocation of histone H1 during the HeLa cell cycle. Chromosoma *108*, 308–316.

Cecconi, F., Alvarez-Bolado, G., Meyer, B.I., Roth, K.A., and Gruss, P. (1998). Apaf1 (CED-4 homolog) regulates programmed cell death in mammalian development. Cell *94*, 727–737.

Chadee, D.N., Allis, C.D., Wright, J.A., and Davie, J.R. (1997). Histone H1b phosphorylation is dependent upon ongoing transcription and replication in normal and ras-transformed mouse fibroblasts. J. Biol. Chem. *272*, 8113–8116.

Clarke, A.R., Purdie, C.A., Harrison, D.J., Morris, R.G., Bird, C.C., Hooper, M.L., and Wyllie, A.H. (1993). Thymocyte apoptosis induced by p53-dependent and independent pathways. Nature *362*, 849–852.

Desagher, S., Osen-Sand, A., Nichols, A., Eskes, R., Montessuit, S., Lauper, S., Maundrell, K., Antonsson, B., and Martinou, J.C. (1999). Bid-induced conformational change of Bax is responsible for mitochondrial cytochrome *c* release during apoptosis. J. Cell Biol. *144*, 891–901.

Ellerby, H.M., Arap, W., Ellerby, L.M., Kain, R., Andrusiak, R., Rio, G.D., Krajewski, S., Lombardo, C.R., Rao, R., Ruoslahti, E., et al. (1999). Anti-cancer activity of targeted pro-apoptotic peptides. Nat. Med. *5*, 1032–1038.

Epand, R.F., Martinou, J.C., Fornallaz-Mulhauser, M., Hughes, D.W., and Epand, R.M. (2002). The apoptotic protein tBid promotes leakage by altering membrane curvature. J. Biol. Chem. *277*, 32632–32639.

Esposti, M.D., Erler, J.T., Hickman, J.A., and Dive, C. (2001). Bid, a widely expressed proapoptotic protein of the Bcl-2 family, displays lipid transfer activity. Mol. Cell. Biol. *21*, 7268–7276.

Fan, Y., Sirotkin, A., Russell, R.G., Ayala, J., and Skoultchi, A.I. (2001). Individual somatic H1 subtypes are dispensable for mouse development even in mice lacking the H1(0) replacement subtype. Mol. Cell. Biol. *21*, 7933–7943.

Flores, E.R., Tsai, K.Y., Crowley, D., Sengupta, S., Yang, A., McKeon, F., and Jacks, T. (2002). p63 and p73 are required for p53-dependent apoptosis in response to DNA damage. Nature *416*, 560–564.

Franke, K., Drabent, B., and Doenecke, D. (1998). Expression of murine H1 histone genes during postnatal development. Biochim. Biophys. Acta *1398*, 232–242.

Fukuda, M., Asano, S., Nakamura, T., Adachi, M., Yoshida, M., Yanagida, M., and Nishida, E. (1997). CRM1 is responsible for intracellular transport mediated by the nuclear export signal. Nature *390*, 308–311.

Griffiths, G.J., Dubrez, L., Morgan, C.P., Jones, N.A., Whitehouse, J., Corfe, B.M., Dive, C., and Hickman, J.A. (1999). Cell damage-induced conformational changes of the pro-apoptotic protein Bak in vivo precede the onset of apoptosis. J. Cell Biol. *144*, 903–914.

Gross, A., Jockel, J., Wei, M.C., and Korsmeyer, S.J. (1998). Enforced dimerization of BAX results in its translocation, mitochondrial dysfunction and apoptosis. EMBO J. *17*, 3878–3885.

Karuman, P., Gozani, O., Odze, R.D., Zhou, X.C., Zhu, H., Shaw, R., Brien, T.P., Bozzuto, C.D., Ooi, D., Cantley, L.C., and Yuan, J. (2001). The Peutz-Jegher gene product LKB1 is a mediator of p53-dependent cell death. Mol. Cell *7*, 1307–1319.

Knudson, C.M., Tung, K.S., Tourtellotte, W.G., Brown, G.A., and Korsmeyer, S.J. (1995). Bax-deficient mice with lymphoid hyperplasia and male germ cell death. Science *270*, 96–99.

Kratzmeier, M., Albig, W., Meergans, T., and Doenecke, D. (1999). Changes in the protein pattern of H1 histones associated with apoptotic DNA fragmentation. Biochem. J. *337*, 319–327.

Lennox, R.W., and Cohen, L.H. (1983). The histone H1 complements of dividing and nondividing cells of the mouse. J. Biol. Chem. *258*, 262–268.

Li, H., Kolluri, S.K., Gu, J., Dawson, M.I., Cao, X., Hobbs, P.D., Lin, B., Chen, G., Lu, J., Lin, F., et al. (2000). Cytochrome *c* release and apoptosis induced by mitochondrial targeting of nuclear orphan receptor TR3. Science *289*, 1159–1164.

Lindsten, T., Ross, A.J., King, A., Zong, W.X., Rathmell, J.C., Shiels, H.A., Ulrich, E., Waymire, K.G., Mahar, P., Frauwirth, K., et al. (2000). The combined functions of proapoptotic Bcl-2 family members Bak and Bax are essential for normal development of multiple tissues. Mol. Cell *6*, 1389–1399.

Lowe, S.W., Schmitt, E.M., Smith, S.W., Osborne, B.A., and Jacks, T. (1993a). p53 is required for radiation-induced apoptosis in mouse thymocytes. Nature *362*, 847–849.

Lowe, S.W., Ruley, H.E., Jacks, T., and Housman, D.E. (1993b). p53-dependent apoptosis modulates the cytotoxicity of anticancer agents. Cell *74*, 957–967.

Majumder, P.K., Pandey, P., Sun, X., Cheng, K., Datta, R., Saxena, S., Kharbanda, S., and Kufe, D. (2000). Mitochondrial translocation of protein kinase C δ in phorbol ester-induced cytochrome *c* release and apoptosis. J. Biol. Chem. *275*, 21793–21796.

Marchenko, N.D., Zaika, A., and Moll, U.M. (2000). Death signal-induced localization of p53 protein to mitochondria. A potential role in apoptotic signaling. J. Biol. Chem. *275*, 16202–16212.

Matsuoka, Y., Takechi, S., Nakayama, T., and Yoneda, Y. (1994). Exogenous histone H1 injection into mitotic cells disrupts synchronous progression of mitotic events by delaying chromosome decondensation. J. Cell Sci. *107*, 693–701.

Miyashita, T., and Reed, J.C. (1995). Tumor suppressor p53 is a direct transcriptional activator of the human bax gene. Cell *80*, 293–299.

Nakano, K., and Vousden, K.H. (2001). PUMA, a novel proapoptotic gene, is induced by p53. Mol. Cell *7*, 683–694.

Oda, E., Ohki, R., Murasawa, H., Nemoto, J., Shibue, T., Yamashita, T., Tokino, T., Taniguchi, T., and Tanaka, N. (2000a). Noxa, a BH3-only member of the Bcl-2 family and candidate mediator of p53-induced apoptosis. Science *288*, 1053–1058.

Oda, K., Arakawa, H., Tanaka, T., Matsuda, K., Tanikawa, C., Mori, T., Nishimori, H., Tamai, K., Tokino, T., Nakamura, Y., and Taya, Y. (2000b). p53AIP1, a potential mediator of p53-dependent apoptosis, and its regulation by Ser-46-phosphorylated p53. Cell *102*, 849–862.

Pepe, I., Catasti, P., Rauch, G., Nizzari, M., and Nicolini, C. (1990). The histone H1 globular region. A possible supersecondary structure from spectroscopic and statistical studies. Biochim. Biophys. Acta *1041*, 14–21.

Polyak, K., Xia, Y., Zweier, J.L., Kinzler, K.W., and Vogelstein, B. (1997). A model for p53-induced apoptosis. Nature *389*, 300–305.

Pritchard, D.M., Potten, C.S., Korsmeyer, S.J., Roberts, S., and Hickman, J.A. (1999). Damage-induced apoptosis in intestinal epithelia from bcl-2-null and bax-null mice: investigations of the mechanistic determinants of epithelial apoptosis in vivo. Oncogene *18*, 7287–7293.

Puthalakath, H., and Strasser, A. (2002). Keeping killers on a tight leash: transcriptional and post-translational control of the pro-apoptotic activity of BH3-only proteins. Cell Death Differ. *9*, 505–512.

Rogakou, E.P., Boon, C., Redon, C., and Bonner, W.M. (1999). Megabase chromatin domains involved in DNA double-strand breaks in vivo. J. Cell Biol. *146*, 905–916.

Rosette, C., and Karin, M. (1996). Ultraviolet light and osmotic stress: activation of the JNK cascade through multiple growth factor and cytokine receptors. Science *274*, 1194–1197.

Shimizu, S., Eguchi, Y., Kamiike, W., Matsuda, H., and Tsujimoto, Y. (1996). Bcl-2 expression prevents activation of the ICE protease cascade. Oncogene *12*, 2251–2257.

Shimizu, S., Eguchi, Y., Kamiike, W., Funahashi, Y., Mignon, A., Lacronique, V., Matsuda, H., and Tsujimoto, Y. (1998). Bcl-2 prevents apoptotic mitochondrial dysfunction by regulating proton flux. Proc. Natl. Acad. Sci. USA *95*, 1455–1459.

Tanaka, M., Hennebold, J.D., Macfarlane, J., and Adashi, E.Y. (2001). A mammalian oocyte-specific linker histone gene H1oo: homology with the genes for the oocyte-specific cleavage stage histone (cs-H1) of sea urchin and the B4/H1M histone of the frog. Development *128*, 655–664.

Tanaka, N., Ishihara, M., Lamphier, M.S., Nozawa, H., Matsuyama, T., Mak, T.W., Aizawa, S., Tokino, T., Oren, M., and Taniguchi, T. (1996). Cooperation of the tumour suppressors IRF-1 and p53 in response to DNA damage. Nature *382*, 816–818.

Tsujimoto, Y. (2003). Cell death regulation by the Bcl-2 protein family in the mitochondria. J. Cell. Physiol. *195*, 158–167.

Tsujimoto, Y., and Shimizu, S. (2000). Bcl-2 family: Life-or-death switch. FEBS Lett. *466*, 6–10.

Vignali, M., and Workman, J.L. (1998). Location and function of linker histones. Nat. Struct. Biol. *5*, 1025–1028.

Vila, R., Ponte, I., Jimenez, M.A., Rico, M., and Suau, P. (2000). A helix-turn motif in the C-terminal domain of histone H1. Protein Sci. *9*, 627–636.

Wang, X. (2001). The expanding role of mitochondria in apoptosis. Genes Dev. *15*, 2922–2933.

Wang, Z.F., Sirotkin, A.M., Buchold, G.M., Skoultchi, A.I., and Marzluff, W.F. (1997). The mouse histone H1 genes: gene organization and differential regulation. J. Mol. Biol. *271*, 124–138.

Wei, M.C., Lindsten, T., Mootha, V.K., Weiler, S., Gross, A., Ashiya, M., Thompson, C.B., and Korsmeyer, S.J. (2000). tBID, a membrane-targeted death ligand, oligomerizes BAK to release cytochrome *c*. Genes Dev. *14*, 2060–2071.

Wei, M.C., Zong, W.X., Cheng, E.H., Lindsten, T., Panoutsakopoulou, V., Ross, A.J., Roth, K.A., MacGregor, G.R., Thompson, C.B., and Korsmeyer, S.J. (2001). Proapoptotic BAX and BAK: a requisite gateway to mitochondrial dysfunction and death. Science *292*, 727–730.

Westphal, C.H., Rowan, S., Schmaltz, C., Elson, A., Fisher, D.E., and Leder, P. (1997). ATM and p53 cooperate in apoptosis and suppression of tumorigenesis, but not in resistance to acute radiation toxicity. Nat. Genet. *16*, 397–401.

Wolf, B.B., and Green, D.R. (2002). Apoptosis: letting slip the dogs of war. Curr. Biol. *12*, R177–R179.

Wolter, K.G., Hsu, Y.T., Smith, C.L., Nechushtan, A., Xi, X.G., and Youle, R.J. (1997). Movement of Bax from the cytosol to mitochondria during apoptosis. J. Cell Biol. *139*, 1281–1292.

Yamaguchi, H., and Wang, H.G. (2002). Bcl-xL protects BimEL-induced Bax conformational change and cytochrome *c* release independent of interacting with Bax or BimEL. J. Biol. Chem. *277*, 41604–41612.

Yoshida, H., Kong, Y.Y., Yoshida, R., Elia, A.J., Hakem, A., Hakem, R., Penninger, J.M., and Mak, T.W. (1998). Apaf1 is required for mitochondrial pathways of apoptosis and brain development. Cell *94*, 739–750.

Yu, J., Zhang, L., Hwang, P.M., Kinzler, K.W., and Vogelstein, B. (2001). PUMA induces the rapid apoptosis of colorectal cancer cells. Mol. Cell *7*, 673–682.

Zoratti, M., and Szabo, I. (1995). The mitochondrial permeability transition. Biochim. Biophys. Acta *1241*, 139–176.